

## Crystal and magnetic structures of $\text{Bi}_2\text{CuO}_4$

This article has been downloaded from IOPscience. Please scroll down to see the full text article.

1990 J. Phys.: Condens. Matter 2 2205

(<http://iopscience.iop.org/0953-8984/2/9/010>)

View [the table of contents for this issue](#), or go to the [journal homepage](#) for more

Download details:

IP Address: 171.66.16.103

The article was downloaded on 11/05/2010 at 05:48

Please note that [terms and conditions apply](#).

## Crystal and magnetic structures of $\text{Bi}_2\text{CuO}_4$

J L García-Muñoz<sup>†</sup>, J Rodríguez-Carvajal<sup>†</sup>, F Sapiña<sup>‡</sup>, M J Sanchis<sup>‡</sup>,  
R Ibáñez<sup>‡</sup> and D Beltrán-Porter<sup>‡</sup>

<sup>†</sup> Institut Laue–Langevin, 156X 38042-Grenoble, France

<sup>‡</sup> Departamento de Química Inorgánica, Universitat de Valencia, UIBCM, Dr Moliner  
50, 46100-Burjassot, Spain

Received 21 July 1989, in final form 10 October 1989

**Abstract.** The crystal structure of  $\text{Bi}_2\text{CuO}_4$  has been reinvestigated and its magnetic structure solved by neutron powder diffraction. The crystal structure, according to earlier work, is perfectly described in the space group  $P4/ncc$ . Contrary to the dimeric magnetic behaviour suggested in a recent paper, the title compound becomes long-range antiferromagnetically ordered below 50 K. The ground state has  $C_2$  symmetry and the crystallographic magnetic group is  $P4/n'c'c'$ . The magnetic moment of copper atoms at 1.5 K is  $0.93(6)\mu_B$ , which is very close to the saturation moment of spin-only Cu(II) ( $d^9$ ).

### 1. Introduction

The magnetic properties of copper oxides are of renewed interest owing to their relationship to the recently discovered high- $T_c$  superconductors; some current theories claim a pairing mechanism of magnetic origin (see, e.g., [1]). In many semiconductor copper oxides directly related to high- $T_c$  superconductors (oxygen-deficient 1:2:3 compounds,  $\text{La}_2\text{CuO}_4$ ), three-dimensional (3D) antiferromagnetic ordering exists as a ground state, in spite of the low dimensionality and the anisotropic super-exchange pathways expected from the crystal structure (see, e.g., [2]). The  $\text{Bi}_2\text{CuO}_4$  system may represent a similar situation as long as the published magnetic data (susceptibility and EPR) [3–5] are not clearly related to the structural data [6, 7].

The structure of  $\text{Bi}_2\text{CuO}_4$  has not been unambiguously resolved. Two space groups have been proposed from x-ray diffraction data on single crystals:  $I4$  [6] and  $P4/ncc$  [7]. The structure in both models can be roughly described as staggered stacking of  $\text{CuO}_4$  square planar units, forming chains along the  $c$  axis inter-connected through  $\text{BiO}_2$  chains. In the  $I4$  symmetry there are two non-equivalent crystallographic sites for copper atoms, leading to alternating Cu–Cu distances along the  $c$  axis. In the  $P4/ncc$  symmetry there is only one crystallographic site for copper atoms, and a unique Cu–Cu distance along the  $c$  axis.

Electron diffraction experiments have been performed [3] on small single crystals of  $\text{Bi}_2\text{CuO}_4$ . The analysis of the electron diffraction patterns gives no conclusive result for the true symmetry, because it was found that there were extra spots not allowed by either the  $I4$  or the  $P4/ncc$  space groups. By looking at the patterns presented, we can draw a straightforward conclusion that the  $I4$  symmetry cannot be correct, since the

presence of forbidden reflections of a non-primitive unit cell cannot be a consequence of multiple scattering. For just the opposite reason the  $P4/ncc$  symmetry cannot be ruled out.

The behaviour of magnetic susceptibility with temperature shows a maximum near 50 K and a minimum around 20 K. The product  $\chi T$  decreases continuously when the temperature is lowered, indicating the presence of antiferromagnetic interactions. In [3] the data were fitted to a uniform antiferromagnetic spin- $\frac{1}{2}$  Heisenberg chain, but this model cannot fit the low-temperature data. The data did not fit the magnetic susceptibility over the entire measured temperature range assuming dimeric units with a nearly degenerate second singlet state close to the ground state. To explain this behaviour, it is necessary to assume the existence of two non-equivalent crystallographic sites for copper atoms. Consequently, the data support the  $I4$  instead of the  $P4/ncc$  symmetry. A recent EPR study [5] does not provide definite evidence for the presence of a spin triplet state nor does it support the possibility of long-range antiferromagnetic order.

The reported studies do not resolve the ambiguities regarding the crystal structure and the range and dimensionality of the magnetic interactions in  $\text{Bi}_2\text{CuO}_4$ . In order to obtain a deeper insight into the understanding of the structural and magnetic properties of  $\text{Bi}_2\text{CuO}_4$ , we have carried out a neutron powder diffraction experiment. Neutron diffraction is more sensitive to oxygen positions, and small departures from a given symmetry can be detected more easily. Moreover the evolution of the diffraction pattern with temperature allows the search for a structural phase transition at low temperatures related to the spin-Peierls dimerisation. From the magnetic point of view, any kind of long-range magnetic ordering can be revealed.

## 2. Experimental details

The phase diagram of the system  $\text{Bi}_2\text{O}_3$ – $\text{CuO}$  was studied in [8] and verified in [9]. The mixed oxide  $\text{Bi}_2\text{CuO}_4$  is a unique compound in the system. It melts congruently at 840 °C and decomposes at temperatures higher than 900 °C.

Taking into account these facts, a sample of  $\text{Bi}_2\text{CuO}_4$  was prepared from stoichiometric amounts of pure  $\text{Bi}_2\text{O}_3$  and  $\text{CuO}$ . Powdered solids were thoroughly mixed by centrifugal milling in a Fritch-Pulverisette for 30 min using isopropyl alcohol as the dispersive medium. The resulting powder was fired in an alumina boat at 750 °C for 32 h with an intermediate grinding. X-ray powder diffraction data were acquired using a Kristalloflex 810 Siemens automatic diffractometer with monochromated  $\text{Cu K}\alpha$  radiation. The experimental pattern corresponded to a single phase and was fully indexed in the  $P4/ncc$  space group. The determination of the atomic positions using a Rietveld analysis of the x-ray pattern profile was nevertheless unsuccessful because of the great difference between the scattering factors of Bi and O and the failure to prepare samples without any preferred orientation. Hereafter, references to diffraction patterns refer to neutron diffraction.

Neutron powder diffraction experiments were performed on the D2B high-resolution powder diffractometer at the Institut Laue–Langevin in Grenoble. About 15 g of powdered  $\text{Bi}_2\text{CuO}_4$  sample was used for the experiment. The sample was put into a cylindrical vanadium can ( $D = 8$  mm;  $h = 6$  cm) and introduced into a helium cryostat. The temperature was computer controlled and its stability during the measurements was better than 0.1 K.

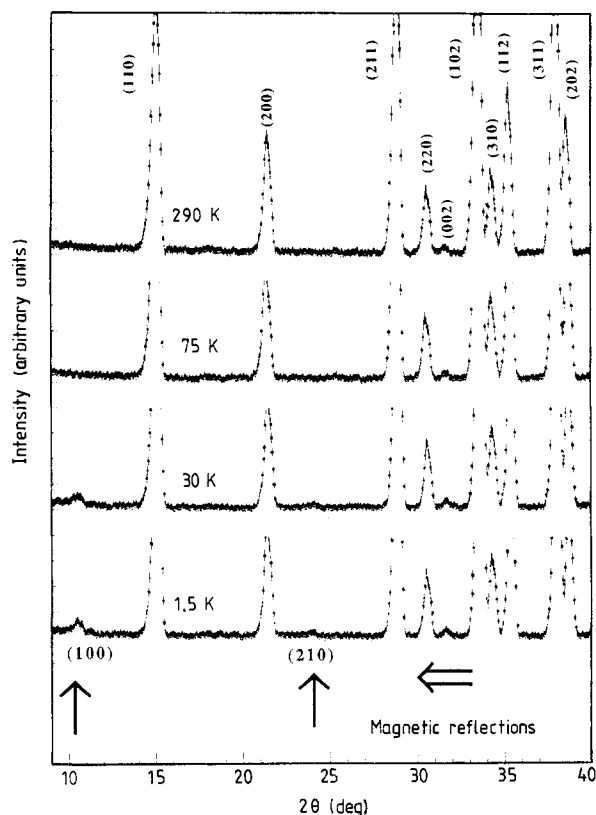


**Figure 1.** Thermal evolution of the small-angle part of the neutron diffraction pattern of  $\text{Bi}_2\text{CuO}_4$ .

The D2B was used in its high-flux mode of operation which gives resolution good enough for our problem and diminishes the difficulties of handling complicated peak shapes due to monochromator defects. The step size for this experiment was  $0.05^\circ$  in  $2\theta$ . The explored angular range was  $0$ – $160^\circ$  ( $2\theta$ ) and the preselected monitor counts, for a fixed position of the detector bank, was 150 000.

Four diffraction patterns were collected at the temperatures 1.5, 30, 75 and 290 K. The analysis of the data was performed using the programs existing in the STRAP package [10]. Instead of using the integrated intensities (or a set of structure factors), the refinements of the crystal and magnetic structures were carried out using the Rietveld method [11]. The full profile is used to fit the structural and magnetic model, minimising by least squares the quantity:  $S = \sum_i w_i [y_i(\text{obs}) - y_i(\text{calc})]^2$ , where  $y_i$  represent the number of counts observed (or calculated) at point of scattering angle  $2\theta_i$  (see [11] for details concerning the method and reliability factors). The neutron wavelength used in the refinements was  $1.5946 \text{ \AA}$ .

### 3. Results

From the neutron diffraction patterns, the main difference between them is the appearance at 1.5 and 30 K of two small reflections which correspond to the (100) and (210) reflections, which are absent at 75 and 290 K. In figure 1 a small portion of the diffraction

patterns are shown as a function of temperature. The fact that these reflections appear only at the low-temperature side of the maximum susceptibility suggest their magnetic origin. This result implies that long-range magnetic ordering is established in this compound. The observed susceptibility maximum reflects, consequently, the transition to a 3D antiferromagnetically ordered state. The increase in the magnetic susceptibility (see figure 3 of [3]) at low temperatures may be due to a paramagnetic impurity.

With this overall result in mind, we have refined the crystal structure on the basis of the previously proposed models [6, 7]. For all the four temperatures, the space group  $P4/ncc$  adequately describes the structure. The simplicity of the structure and the low number of positional parameters to fit have allowed the refinement of the anisotropic thermal parameters of all the atoms. Table 1 shows the relevant crystallographic parameters and the reliability factors of the refinements for each temperature. Figure 2 is an example of the Rietveld refinement performed for the 30 K case, showing the observed, calculated and difference patterns as well as the Bragg reflections markers. In the refinements we have not taken into account the weak magnetic reflections, since their effect on the nuclear structure is negligible. In figure 3 a  $[001]$  projection of the structure is shown.

Because copper atoms are located on sites  $4c$  of point symmetry 4 for the whole temperature range explored, the admissible magnetic point group of the sites is also 4. Therefore the only admissible spin direction is  $[001]$  [12]. The spin direction along the  $c$  axis is also corroborated by the fact that the strongest magnetic reflections have  $l = 0$ . As there are only four copper cations in the unit cell, and on the assumption that the magnetic moments are parallel to the  $c$  axis, it is straightforward to find the magnetic structure of this compound. We can divide the copper atoms into four equivalent sublattices according to the numbering Cu(1),  $(\frac{1}{4}, \frac{1}{4}, z)$ ; Cu(2),  $(\frac{1}{4}, \frac{1}{4}, z + \frac{1}{2})$ ; Cu(3),

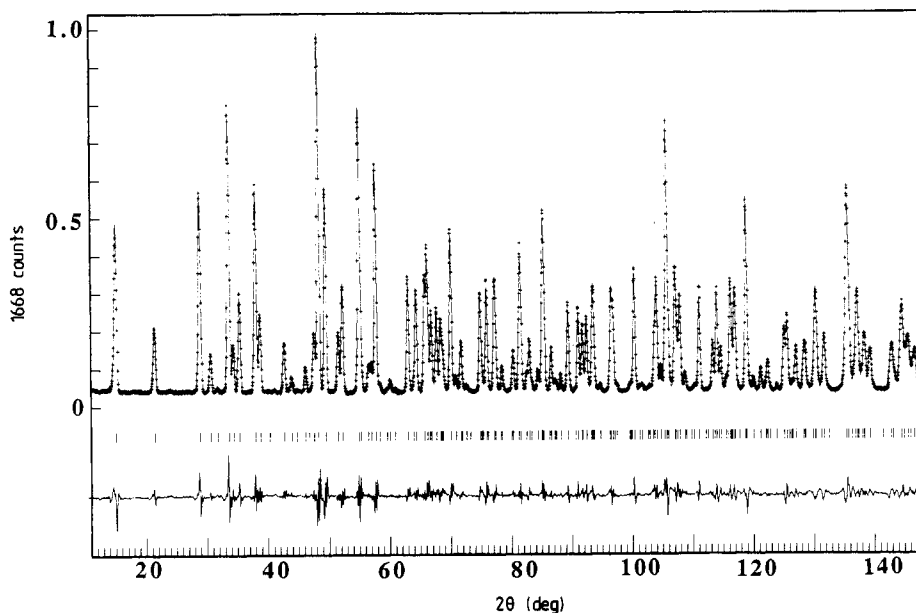


**Figure 2.** Observed and calculated neutron diffraction patterns of  $\text{Bi}_2\text{CuO}_4$  at 30 K: +, observed counts; —, calculated pattern. The curve at the bottom is the difference pattern  $y(\text{obs}) - y(\text{calc})$ ; the small bars indicate the angular positions of the allowed Bragg reflections.

**Table 1.** Crystallographic parameters.

<i>t</i>	Value at the following temperatures			
	1.5 K	30 K	75 K	290 K
Cell parameters (Å)				
<i>a</i>	8.4989(1)	8.4988(1)	8.4987(1)	8.5039(1)
<i>c</i>	5.7973(1)	5.7976(1)	5.7999(1)	5.8202(1)
Atom coordinates: Space group $P4/ncc$ , origin at centre $-\bar{1}$				
Bi (8f): ( <i>x</i> , $-x$ , $\frac{3}{4}$ )				
Cu (4c): ( $\frac{1}{4}$ , $\frac{1}{4}$ , <i>z</i> )				
O (16g): ( <i>x</i> , <i>y</i> , <i>z</i> )				
<i>x</i> (Bi)	0.0817(1)	0.0817(1)	0.0818(1)	0.0814(1) <i>0.0815(2)</i>
<i>z</i> (Cu)	0.0766(3)	0.0764(3)	0.0765(3)	0.0770(3) <i>0.080(4)</i>
<i>x</i> (O)	0.5500(1)	0.5501(1)	0.5500(1)	0.5498(1) <i>0.545(4)</i>
<i>y</i> (O)	-0.1421(1)	-0.1422(1)	-0.1421(1)	-0.1424(1) <i>-0.136(4)</i>
<i>z</i> (O)	-0.0913(2)	-0.0915(2)	-0.0911(2)	-0.0914(2) <i>-0.097(4)</i>
Number of reflections				
	194	194	194	196
Scale	0.484(2)	0.484(2)	0.484(2)	0.482(2)
<i>U</i>	0.077(2)	0.080(2)	0.079(2)	0.077(2)
<i>V</i>	-0.165(5)	-0.171(5)	-0.171(5)	-0.186(5)
<i>W</i>	0.229(3)	0.231(3)	0.232(3)	0.239(2)
$\eta$	0.110(7)	0.108(7)	0.109(7)	0.082(7)
Asymmetric	0.86(3)	0.87(3)	0.85(3)	0.92(3)
Reliability factors				
$R_{wp}$	7.65	7.58	7.39	6.81
$R_E$	2.97	2.97	2.96	2.97
$R_{Bragg}$	2.59	2.61	2.51	2.86
Thermal parameters ( $\times 10^5$ ) according to the expression $\exp[-(h^2\beta_{11} + k^2\beta_{22} + l^2\beta_{33} + 2hk\beta_{12} + 2hl\beta_{13} + 2kl\beta_{23})]$				
Bi (8f)				
$\beta_{11} = \beta_{22}$	72(6)	79(6)	101(6)	227(6)
$\beta_{33}$	191(23)	221(23)	270(23)	660(26)
$\beta_{12}$	9(11)	10(11)	10(11)	15(12)
$\beta_{13} = \beta_{23}$	16(12)	29(12)	11(12)	14(13)
$B_{eq}$ (Å <sup>2</sup> )	0.224	0.251	0.316	0.736
Cu (4c)				
$\beta_{11} = \beta_{22}$	77(11)	83(11)	84(11)	189(11)
$\beta_{33}$	349(36)	340(36)	414(36)	688(38)
$\beta_{12} = \beta_{13} = \beta_{23} = 0$				
$B_{eq}$ (Å <sup>2</sup> )	0.305	0.312	0.348	0.675
O (16g)				
$\beta_{11}$	136(14)	136(14)	154(14)	293(15)
$\beta_{22}$	135(14)	137(13)	154(13)	269(14)
$\beta_{33}$	371(23)	389(23)	455(23)	843(25)
$\beta_{12}$	4(9)	-3(9)	3(9)	39(9)
$\beta_{13}$	-3(18)	14(18)	-10(18)	25(20)
$\beta_{23}$	6(15)	12(15)	-5(15)	39(16)
$B_{eq}$ (Å <sup>2</sup> )	0.331	0.341	0.404	0.730

Values in italics correspond to the values in [5] adapted to our origin setting. Reliability factors used here are described in [11].

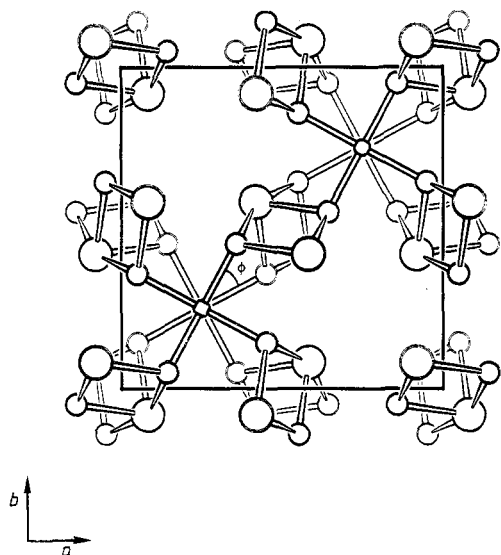


**Figure 3.** Structure of  $\text{Bi}_2\text{CuO}_4$  along  $[001]$ . The large open circles are Bi atoms, the small open circles are Cu atoms and the intermediate open circles are O atoms. The twist angle  $\varphi$  is displayed.

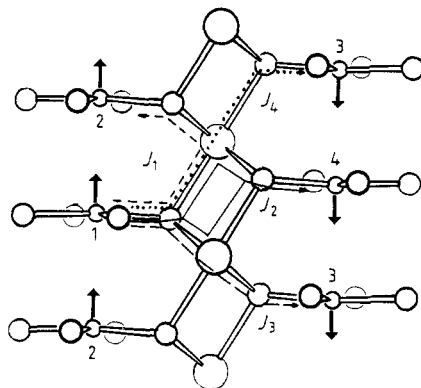


**Figure 4.** Magnetic structure of  $\text{Bi}_2\text{CuO}_4$ . The structure is drawn as seen along the  $[1\bar{1}0]$  direction. The exchange pathways are also displayed.

$(\frac{3}{4}, \frac{3}{4}, \frac{1}{2}-z)$ ;  $\text{Cu}(4), (\frac{3}{4}, \frac{3}{4}, -z)$ . The only possible independent modes are

$$\begin{aligned} F_z: S_1 + S_2 + S_3 + S_4 & & C_2: S_1 + S_2 - S_3 - S_4 \\ G_z: S_1 - S_2 + S_3 - S_4 & & A_2: S_1 - S_2 - S_3 + S_4. \end{aligned}$$

The magnetic structure factor for the spin arrangements can be written as

$$F_m(Q) = (A + \eta_2 A e^{\pi i l} + \eta_3 A^* + \eta_4 A^* e^{-\pi i l}) f(Q) S$$

where  $A = e^{i\pi(h+k)/2} e^{2\pi i z l}$ ,  $f(Q)$  is the magnetic form factor of Cu atoms,  $S$  is the magnetic moment on Cu atoms and  $\eta_i = \pm 1 (i=2, \dots, 4)$  are factors determining the sign of the spin  $S_i$  in each independent mode:  $S_1 + \sum_{i=2}^4 \eta_i S_i$ .

Taking into account the above magnetic structure factor, it is easy to find the conditions limiting possible magnetic reflections. For a given  $(hkl)$ ,  $l$  is even for modes F and C and odd for modes A and G. The modes A and G have to be discarded since the two indexed magnetic peaks (100 and 210) have even  $l$ -values. Moreover, for reflections  $(hk0)$  the conditions limiting possible magnetic reflections for modes F and C are  $h+k=2n$  and  $h+k=2n+1$ , respectively. These simple considerations determine unambiguously the solution to be mode C.

This mode corresponds to a ferromagnetic intra-chain coupling and antiferromagnetic inter-chain coupling, as pictured in figure 4. The crystallographic magnetic group is  $P4/n'c'c'$ .

To obtain the magnetic moment of copper atoms, a Rietveld refinement of the magnetic structure was done using a locally modified version of the original Rietveld program. Only a restricted angular range ( $2\theta = 9-50^\circ$ ) was used owing to the weakness of magnetic reflections. For this reason the crystallographic parameters were fixed to the values obtained with the 'nuclear-only' full pattern refinement. In this angular range there exist 24 reflections, of which five are purely magnetic (100, 210, 300, 320 and 410),

**Table 2.** Calculated nuclear and magnetic intensities compared with the observed values at small angles ( $2\theta < 50^\circ$ ) for  $\text{Bi}_2\text{CuO}_4$  at 1.5 K.

$h$	$k$	$l$	$I_{\text{nuc}}$	$I_{\text{mag}}$	$I_{\text{obs}}$
1	0	0	0	262	299
1	1	0	7733	0	7358
2	0	0	2722	0	2939
2	1	0	0	86	86
2	1	1	7982	0	8629
2	2	0	1520	0	1646
0	0	2	80	0	190
3	0	0	0	20	29
1	0	2	11949	1	12091
3	1	0	1799	0	1814
1	1	2	3934	0	4020
3	1	1	8485	0	8594
2	0	2	3025	5	3060
3	2	0	0	23	16
2	1	2	8	5	11
3	2	1	2030	0	2054
4	0	0	556	0	602
2	2	2	64	5	67
4	1	0	0	15	15
3	0	2	996	2	930
3	3	0	3	0	4
3	1	2	2215	9	2449
4	1	1	14281	0	14192
4	2	0	8323	0	8063
$R$ -factor (nuclear)			3.27		
$R$ -factor (magnetic)			11.34		

six have a small magnetic contribution and the remaining are pure nuclear reflections. As an example, in table 2 we give the observed and calculated integrated intensities at 1.5 K. The only relevant refined parameter was the magnetic moment of copper atoms. The result was  $\mu(\text{Cu}) = 0.93(6)\mu_{\text{B}}$  at 1.5 K ( $R_{\text{mag}} = 11.34$ ) and  $\mu(\text{Cu}) = 0.81(7)\mu_{\text{B}}$  at 30 K ( $R_{\text{mag}} = 15.46$ ). The relatively high values of the  $R$ -factors depend strongly on the background level owing to the weakness of the magnetic reflections. However, the calculated magnetic moments are not affected by this problem.

#### 4. Discussion

From a purely crystallographic point of view, our results fully support the previous findings in [7]. The space group  $\text{P4}/ncc$  is correct. The small differences between the atom coordinates in [7] and our corresponding values arise because, with x-rays, the scattering power of Bi atoms is very high with respect to oxygen atoms, and therefore the position parameters of the light atoms given in [7] are somewhat inaccurate. In table 3 we give the more relevant distances and angles as a function of temperature in  $\text{Bi}_2\text{CuO}_4$ .

In the full range of temperatures studied, no particular distortion or structural phase transition is detected. The variation in cell and positional parameters with respect to the



**Table 3.** Relevant distances and angles for  $\text{Bi}_2\text{CuO}_4$ .

	Values at the following temperatures			
	1.5 K	30 K	75 K	290 K
Cu–O ( $\times 4$ ) (Å)	1.9328(9)	1.9322(9)	1.9331(9)	1.9348(9)
Bi–O ( $\times 2$ ) (Å)	2.131(1)	2.130(1)	2.131(1)	2.133(1)
( $\times 2$ ) (Å)	2.331(1)	2.332(1)	2.331(1)	2.337(1)
Cu–Cu ( $\times 2$ ) (Å)	2.899(3)	2.899(3)	2.900(3)	2.910(3)
$\varphi$ (deg)	33.31(3)	33.33(3)	33.31(3)	33.49(3)
O–Cu–O ( $\times 4$ ) (deg)	89.89(3)	89.88(3)	89.89(3)	89.89(3)
O–Cu–O ( $\times 2$ ) (deg)	175.0(1)	174.8(1)	175.0(1)	175.0(1)
O–Bi–O ( $\times 2$ ) (deg)	76.66(4)	76.70(4)	76.61(4)	76.69(4)
O–Bi–O ( $\times 2$ ) (deg)	88.02(5)	87.98(5)	88.05(5)	88.28(5)
O–Bi–O (deg)	87.74(5)	87.76(5)	87.76(5)	87.82(5)
O–Bi–O (deg)	158.79(5)	158.79(5)	158.76(5)	159.18(5)

temperature is smooth and very small. For instance, the difference between extreme values of cell parameters are about 0.06% for the  $a$  axis and 0.4% for the  $c$  axis. The variation in thermal parameters with temperature is also normal, but we need some other measurements at higher temperatures in order to know whether our values for them are affected by static disorder or not.

The crystal structure is characterised by the presence of only one type of copper atom in square-planar coordination. Cu is slightly displaced (0.085 Å) from the plane defined by its four bonded oxygen atoms. Square units  $\text{CuO}_4$  form staggered chains along the  $c$  axis, the twist angle  $\varphi$  being 33.3°.

As pointed out in [7], the Bi atoms can be considered to have, as a coordination polyhedron, a trigonal bipyramid of oxygen atoms in which an equatorial oxygen atom is substituted by the lone pair  $E 6s^2$  of  $\text{Bi}^{3+}$ . The bipyramids  $\text{BiO}_4E$  are linked and share edges, constituting the  $(\text{BiO}_2)_n$  chains along the  $c$  axis.

In this structure there is no cation–anion–cation exchange interactions among the possible exchange pathways. The direct exchange Cu–Cu along the  $\text{CuO}_4$  chains can be ruled out since the smaller distance Cu–Cu at 1.5 K ( $d_{\text{Cu–Cu}} = 2.899(3)$  Å) still seems too large. Super-exchange interactions involving two oxygen atoms have been invoked as being responsible for short-range order interactions along the chains [4], and the staggered geometry of the  $\text{CuO}_4$  units supports the ferromagnetic nature of the exchange through this pathway [4]. The short-range interactions that determine the observed antiferromagnetic behaviour of this compound must then relate copper atoms belonging to different chains.

If we adopt the hypothesis that magnetic interactions in this compound propagate only through the  $\text{BiO}_2$  units, there exist only four inequivalent Cu–O–Bi–O–Cu pathways in the  $\text{Bi}_2\text{CuO}_4$  structure, giving rise to four inequivalent exchange integrals.

(1)  $J_1 = J_{12}$  describes the inter-chain interaction. Each copper atom Cu(1) has two Cu(2) as nearest neighbours at 2.91 Å along the chains. The following exchange integrals describe the inter-chain interactions.

(2)  $J_2 = J_{14}$  describes the interaction of the sublattices 1 and 4. Each copper atom Cu(1) has four Cu(4) nearest neighbours at 6.08 Å.

(3)  $J_3 = J_{13}$ , each copper atom Cu(1) has four Cu(3) nearest neighbours at 6.34 Å.

(4)  $J_4 = J'_{13}$  describes the next-nearest-neighbour interaction between sublattices 1 and 3. Each copper atom Cu(1) has four Cu(3) as next-nearest neighbours at 7.12 Å.

The magnetic interactions are depicted in figure 4. From our experiment there is no *a priori* argument to predict the relative strength of the different exchange integrals. Moreover, the absence of direct (cation–anion–cation) super-exchange interactions prevent the use of arguments based on super-exchange angles, or distances, to predict the sign and strength of the interactions. However, the effective inter-chain interaction must be negative and larger than  $J_1$ , at least at high temperatures, i.e. in order to agree with the experimental susceptibility, which gives a negative paramagnetic Curie temperature indicating predominant antiferromagnetic interactions.

In spite of the limited validity, a molecular field (MF) estimation of the exchange integrals is in agreement with the above statement. This estimation can be done assuming only nearest-neighbour interactions  $J_4 = J'_{13} = 0$  and assuming that  $J_2$  is equal to  $J_3$ . Taking the susceptibility data from [3], we can use the maximum of the susceptibility as an estimate of the Néel point; we have  $T_N \approx 50$  K and  $\Theta \approx -40$  K. The expressions for these quantities in the MF framework, for collinear magnetic structures, can be written as (see, for instance, [13])

$$\Theta = \frac{2S(S+1)}{3k} \sum_{j=1,n} z_{ij} J_{ij} = \frac{\alpha}{k} \sum_{j=1,n} z_{ij} J_{ij}$$

$$T_N = \frac{2S(S+1)}{3k} \sum_{j=1,n} z_{ij} J_{ij} \eta_{ij} = \frac{\alpha}{k} \sum_{j=1,n} z_{ij} J_{ij} \eta_{ij}$$

where  $S$  is the spin,  $k$  is the Boltzmann constant and  $n$  is the number of crystallographically equivalent sublattices needed to describe the interactions in such a way that an atom has no interactions with any neighbour on its own sublattice ( $J_{ii} = 0$ ). This condition is satisfied by our sublattice division:  $z_{ij}$  is the number of neighbours of atom  $i$  belonging to the sublattice  $j$ , and  $\eta_{ij} = \pm 1$  are the signs of the spins corresponding to the particular kind of antiferromagnetic ordering established. With our sublattice division and for mode  $C_2$ , we have

$$\Theta = \alpha(2J_1 + 8J_2)/k \quad T_N = \alpha(2J_1 - 8J_2)/k.$$

Solving for  $J_1$  and  $J_2$  we obtain

$$J_1/k = (\Theta + T_N)/4\alpha \quad J_2/k = (\Theta - T_N)/16\alpha.$$

Taking  $S = \frac{1}{2}$  and substituting the values of  $\Theta$  and  $T_N$ , we obtain the following exchange integrals:  $J_1/k = 5$  K and  $J_2/k = -11.25$  K. The magnetic phase diagram predicted by the simple MF theory for our topology can be easily established in the  $J_1$ – $J_2$  plane: the mode C is stable when  $J_1 > 0$ ,  $J_2 < 0$ , or when  $J_1 < 0$ ,  $J_2 < 0$  but  $J_1 < 2J_2$ . It must be noticed that  $J_1$  would be zero if  $\Theta = -T_N$  but, if  $\Theta < -3T_N$ , the mode A (or G) would be the most favourable.

A more detailed study of the magnetic phase transition on single crystals using a high-flux neutron diffractometer, magnetic susceptibility and specific heat experiments is needed in order to ascertain the nature of the transition and how the 3D magnetic order is established.

## Acknowledgments

We acknowledge partial support from the Comisión Interministerial para la Ciencia y la Tecnología (Spain) through Grant PB86/45.

## References

- [1] Anderson P W 1987 *Science* **235** 1196  
Anderson P W, Baskaran G, Zou Z and Hsu T 1987 *Phys. Rev. Lett.* **58** 2790  
Emery V J 1987 *Phys. Rev. Lett.* **58** 2794  
Aharony A, Birgenau R J, Coniglio A, Kastner M A and Stanley H E 1988 *Phys. Rev. Lett.* **60** 1330
- [2] Tranquada J M et al 1988 *Phys. Rev. Lett.* **60** 156  
Kadowaki H et al 1988 *Phys. Rev. B* **37** 7932  
Endoh Y et al 1988 *Phys. Rev. B* **37** 7443  
Tranquada J M et al 1988 *Phys. Rev. B* **38** 2477  
Sato M et al 1988 *Phys. Rev. Lett.* **61** 1317
- [3] Sreedhar K, Ganguly P and Ramasesha S 1988 *J. Phys. C: Solid State Phys.* **21** 1129
- [4] Sreedhar K and Ganguly P 1988 *Inorg. Chem.* **27** 2261
- [5] Ganguly P, Sreedhar K, Raju A R, Demazeau G and Hagenmuller P 1989 *J. Phys.: Condens. Matter* **1** 213
- [6] Arpe R and Muller-Buschbaum H 1976 *Z. Anorg. Chem.* **426** 1
- [7] Boivin J C, Trehoux J and Thomas D 1976 *Bull. Soc. Fr. Minéral. Cristallogr.* **99** 193
- [8] Boivin J C, Thomas D and Tridot G 1973 *C. R. Acad. Sci. Paris C* **276** 1105
- [9] Kakhan B G, Lazarev V B and Shaplygin I S 1979 *Russ. J. Inorg. Chem.* **24** 922
- [10] Rodríguez J, Anne M and Pannetier J 1987 *Institut Laue-Langevin Internal Report* 87RO14T
- [11] Rietveld H M 1969 *J. Appl. Crystallogr.* **2** 65–71; the program used for the 'nuclear' refinement which is described in [10] is a modification of the program published by Young R A and Wiles D B 1982 *J. Appl. Crystallogr.* **15** 430–8
- [12] Opechowski W and Guccione R 1965 *Magnetism* vol IIA, ed G T Rado and H Suhl (New York: Academic) pp 105–65
- [13] Smart J S 1966 *Effective Field Theories of Magnetism* (Philadelphia, PA: Saunders)